Evidence and manipulation of O-GlcNAcylation in granulosa cells of bovine antral follicles†

Authors: Maucieri, Abigail M., and Townson, David H.

Source: Biology of Reproduction, 104(4) : 914-923

Published By: Society for the Study of Reproduction

URL: https://doi.org/10.1093/biolre/ioab013

Biology of Reproduction, 2021, 104(4), 914–923
doi:10.1093/biolre/ioab013
Research Article
Advance Access Publication Date: 8 February 2021

Research Article

Evidence and manipulation of O-GlcNAcylation in granulosa cells of bovine antral follicles†

Abigail M. Maucieri and David H. Townson*

Department of Animal and Veterinary Sciences, The University of Vermont, Burlington, VT, USA

***Correspondence:** 570 Main Street, Terrill Building, Burlington, VT 05405, USA. E-mail: dave.townson@uvm.edu

†Grant Support: This work was supported by USDA Hatch Funds (AMM), USDA Multi-State Project NE-1727 (DHT), and USDA-AFRI Grant #2020-67016-31018 from the National Institute of Food and Agriculture.

Received 14 September 2020; Revised 2 December 2020; Accepted 26 January 2021

Abstract

Glucose is a preferred energy substrate for metabolism by bovine granulosa cells (GCs). O-linked N-acetylglucosaminylation (O-GlcNAcylation), is a product of glucose metabolism that occurs as the hexosamine biosynthesis pathway (HBP) shunts O-GlcNAc sugars to serine and threonine residues of proteins. O-GlcNAcylation through the HBP is considered a nutrient sensing mechanism that regulates many cellular processes. Yet little is known of its importance in GCs. Here, O-GlcNAcylation in GCs and its effects on GC proliferation were determined. Bovine ovaries from a slaughterhouse, staged to the mid-to-late estrous period were used. Follicular fluid and GCs were aspirated from small (3–5 mm) and large (>10 mm) antral follicles. Freshly isolated GCs of small follicles exhibited greater expression of O-GlcNAcylation and O-GlcNAc transferase (OGT) than large follicles. Less glucose and more lactate was detectable in the follicular fluid of small versus large follicles. Culture of GCs revealed that inhibition of the HBP via the glutamine fructose-6-phosphate aminotransferase inhibitor, DON (50 μM), impaired O-GlcNAcylation and GC proliferation, regardless of follicle size. Direct inhibition of O-GlcNAcylation via the OGT inhibitor, OSMI-1 (50 μM), also prevented proliferation, but only in GCs of small follicles. Augmentation of O-GlcNAcylation via the O-GlcNAcase inhibitor, Thiamet-G (2.5 μM), had no effect on GC proliferation, regardless of follicle size. The results indicate GCs of bovine antral follicles undergo O-GlcNAcylation, and O-GlcNAcylation is associated with alterations of glucose and lactate in follicular fluid. Disruption of O-GlcNAcylation impairs GC proliferation. Thus, the HBP via O-GlcNAcylation constitutes a plausible nutrient-sensing pathway influencing bovine GC function and follicular growth.

Summary sentence: O-GlcNAcylation occurs in granulosa cells of small and large bovine antral follicles, and its inhibition impairs granulosa cell proliferation.

Key words: ovary, bovine, granulosa cell, glucose, metabolism, O-GlcNAcylation.

Introduction

O-linked N-acetylglucosaminylation (O-GlcNAcylation) is a form of post-translational glycosylation of cellular proteins in which sugar moieties are added to serine and threonine residues that might otherwise undergo phosphorylation [1, 2]. The process is highly conserved and occurs through the hexosamine biosynthesis pathway (HBP), an alternate path for glucose metabolism in the cell (Figure 1). As much as 2–5% of all glucose in the cell is metabolized through the HBP. The enzyme, O-GlcNAc transferase (OGT) adds the GlcNAc sugar from the donor substrate, uridine diphosphate N-acetylglucosamine (UDP-GlcNAc), to proteins. Conversely, the enzyme O-GlcNAcase (OGA), removes these same GlcNAc sugars from proteins. These

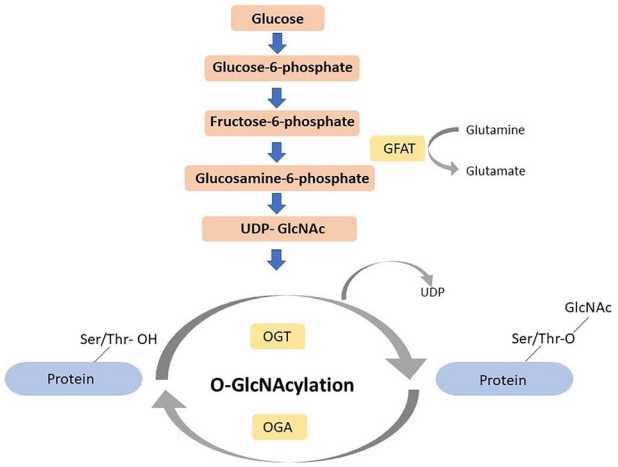

Figure 1. Schematic of glucose metabolism through the hexosamine biosynthesis pathway (HBP) and the process of O-GlcNAcylation. Approximately 2–5% of all glucose metabolized by the cell enters the HBP. Glutamine fructose-6-phosphate aminotransferase (GFAT) is a rate-limiting enzyme of O-GlcNAcylation that partitions fructose-6-phosphate (an intermediate of glycolysis) to form glucosamine-6-phosphate, and ultimately, uridine diphosphate N-acetylglucosamine (UDP-GlcNAc). Subsequently, the enzyme, O-GlcNAc transferase (OGT) adds GlcNAc sugars from the donor substrate, UDP-GlcNAc, to serine/threonine residues of proteins. Conversely, the enzyme O-GlcNAcase (OGA), removes these same GlcNAc sugars from proteins. OGT and OGA enzymes are the sole regulators of O-GlcNAcylation and influence the process in a cyclic manner [1].

two enzymes are the sole regulators of O-GlcNAcylation and influence O-GlcNAcylation in a cyclic manner [1]. The process of O-GlcNAcylation, however, is highly dependent on nutrient availability and is proposed as a nutrient-sensing mechanism within the cell, similar to the functions of AMP-activated protein kinase (AMPK), insulin/IGF-1 signaling (IIS) and mammalian target of rapamycin (mTOR) [3–5]. O-GlcNAcylation regulates cellular processes, including proliferation, signal transduction, and metabolism, and is responsive to many aspects of cellular stress [6]. For instance, O-GlcNAcylation increases as a variety of cell types are exposed to heat stress or hypoxia [6]. This increase in O-GlcNAcylation in response to stress is considered a protective mechanism to maintain cell viability [7]. Additionally, O-GlcNAcylation modulates cellular signaling, similar to phosphorylation, in which various kinases can also be O-GlcNAcylated [8]. Several of the kinases that undergo O-GlcNAcylation and phosphorylation are integral to signaling pathways, including cell growth (ERK5, MAPK14, STK24/25), cell cycle progression (CDK2, casein kinase 2, CLK), cell proliferation (H11, SRC), cell metabolism (pyruvate kinase, SNARK, protein kinase C), transcription (BRD3), and cell death (STK24) [8].

Several of the nutrient sensing pathways that impact granulosa cell (GC) function and follicular growth include AMPK, IIS, and mTOR. Activation of AMPK hinders FSH and IGF-1 induced GC proliferation, and impairs progesterone and estradiol secretion [9–12]. Stimulation of insulin signaling (IIS) supports GC proliferation and FSH-induced estradiol secretion [13]. Lastly, inhibition of mTOR reduces GC proliferation and impedes follicle growth in vitro [14]. Although O-GlcNAcylation influences cellular processes, its role in ovarian physiology, particularly GC function and follicular growth, has not been studied. Glucose is the preferred energy substrate of GCs, but glucose metabolism in growing follicles remains poorly understood, especially as it pertains to the HBP and alternate pathways of glucose utilization. The possibility exists that the HBP in conjunction with O-GlcNAcylation controls many cellular processes of GCs, including metabolism and proliferation, which are critical for follicular development.

In this study, glucose metabolism and O-GlcNAcylation in the GCs of bovine ovarian follicles were evaluated in the context of the HBP. Our objectives were to assess O-GlcNAcylation in bovine GCs of antral follicles of different sizes (i.e., small and large), and evaluate the effects of O-GlcNAcylation on GC proliferation. We hypothesized that O-GlcNAcylation differs in GCs according to antral follicle size and ultimately influences GC proliferation.

Materials and methods

GC isolation and follicular fluid collection

Pairs of bovine ovaries were collected from a slaughterhouse (Champlain Beef, Whitehall, NY, USA) and transported to the laboratory in 0.9% sterile saline with antibiotic–antimycotic (10, 000 units/mL of penicillin, 10, 000 µg/mL of streptomycin, and 25 µg/mL of Gibco Amphotericin B, Gibco, Gaithersburg, MD, USA) at room temperature for processing within 4–6 h of slaughter. The ovaries were morphologically staged to the estrous cycle based upon the visual appearance of the corpus luteum (Ireland et al., 1980). Only ovaries within the mid-to-late estrous cycle, were used. Small antral follicles (3–5 mm; 12–24 follicles per ovary pair) were aspirated with a 21-gauge needle and 3 mL luer lock syringe, and the GCs were pooled into a single sample. Large antral follicles (>10 mm) were dissected from the ovary and aspirated to obtain GCs in a similar fashion to the small follicles, but only the largest follicle from each ovary pair was aspirated for collection. After aspiration, the large follicles were then sliced and scraped with a 5 mm rubber policeman to obtain additional GCs to pool with the previously obtained aspirates. All samples were centrifuged at 84 × *g* for 10 min at 4°C to separate GCs from the follicular fluid. The follicular fluid was separated, aliquoted, and frozen at −80°C until further analyses were performed. The cell pellets were resuspended in 1X Red Blood Cell Lysis Buffer (#5831, Biovision, Milpitas, CA, USA) to lyse red blood cells (RBC) and centrifuged for 5 min at 84 × *g* to pellet the GCs. Once pelleted, the GCs were then resuspended in phosphate-buffered saline (PBS), and cell suspensions were either prepared for lysis of freshly isolated GCs or placed in cell culture as described below.

Lysis of freshly isolated GCs for electrophoresis and immunoblotting

Suspensions of GCs were centrifuged at 2655 × *g* for 10 min at 4°C, and the PBS wash was repeated. PBS was then removed, and the cells were resuspended in radioimmunoprecipitation assay (RIPA) lysis buffer (20 mM Tris HCl, 150 mM NaCl, 1 mM EDTA, 1 mM EGTA, 1% TritonX 100) with HALT protease/phosphatase inhibitor (Thermo Scientific, Waltham, MA, USA) for 10 min. Each suspension was further lysed via aspiration through a 27-gauge needle (BD, Franklin Lakes, NJ, USA). Samples were vortexed for 15 s and centrifuged at 15, 294 × *g* for 10 min. The protein containing supernatant was removed, diluted in Lamelli sample buffer and boiled at 100°C for 1–3 min. Initial protein quantification and standardization was not performed prior to electrophoresis and immunoblotting because of limited sample abundance. Instead, samples were later normalized to the total protein present within the gels by densitometric analyses prior to electrophoretic transfer and immunoblotting.

GC culture

Bovine GCs were isolated as described above, and the cells from each ovary pair were seeded in culture vessels (Corning, Tewksbury, MA, USA) containing DMEM/F12 culture medium (Gibco), 10% fetal bovine serum (Corning), and an antibiotic–antimycotic mixture (10, 000 units/mL of penicillin, 10, 000 µg/mL of streptomycin, and 25 µg/mL of Gibco Amphotericin B; Gibco), regardless of cell number/viability. The GCs were incubated at 37°C in 5% CO_2 and 95% air until 75% confluent, but no more than 72 h. Typically, a yield of 2–4 × 10^6 cells/ovary pair with >95% viability was obtained using these methods, which then enabled culture in flasks or multiwell plates (i.e., T25 flasks, 12-well, and 96-well plates) for experimentation. At the time of experiments, the cultures were switched to serum-free DMEM/F12 medium that contained reduced concentrations of ITS (insulin-10 ng/mL, transferrin-5.5 ng/mL, and sodium selenite-0.67 pg/mL) and a variety of hormones or small molecule inhibitors (e.g., OSMI-1, Thiamet-G) for the duration of the culture, depending upon the experiment. In initial experiments, we verified that GCs obtained from ovary pairs and cultured in this manner retain a GC phenotype, capable of aromatizing testosterone to estradiol (see supplementary information). In particular, insulin-like growth factor-1 (IGF1) and follicle stimulating hormone (FSH) stimulated GC proliferation (Supplementary Figure S1), cytokines induced apoptosis of GCs (Supplementary Figure S2), and IGF1 + FSH stimulated *STAR*, *FSHR*, and *CY19A1* mRNA expression (Supplementary Figure S3) as well as estradiol secretion, when cultures were supplemented with testosterone (Supplementary Figure S4).

Lysis of cultured GCs for electrophoresis and immunoblotting

For detection of O-GlcNAcylation in cultured cells, the GCs of small and large antral follicles were seeded in T25 flasks and treated without or with the glutamine fructose-6-phosphate aminotransferase (GFAT) inhibitor, DON (50 µM), or the small molecule inhibitors to OGT (OSMI-1; 50 µM) or to OGA (Thiamet-G; 2.5 µM) for 4–24 h using doses described in previously published studies [15, 16]. All inhibitors were sourced from Cayman Chemical (Ann Arbor, MI, USA). As OSMI-1 and Thiamet-G-were reconstituted in dimethyl sulfoxide (DMSO; Fisher Scientific) at 1000X, control cultures of GCs also received 0.1% DMSO. Following treatment, flasks were placed on ice and washed three times with 1 mL PBS prior to lysis of GCs using RIPA buffer. Briefly, PBS was removed from the flasks and 200–500 µL of RIPA lysis buffer was added for 10 min. Flasks were then scraped with a cell scraper to remove the GCs from the bottom of the flasks. The GCs were collected into 1.5 mL microcentrifuge tubes and further lysed by aspirating through a 27-gauge needle (BD). Samples were vortexed for 15 s and centrifuged at 15, 294 × *g* for 10 min. The protein containing supernatant was removed and used for protein standardization using a bicinchoninic acid (BCA) colorimetric assay (Thermo Scientific) following manufacturer's instructions. Absorbance at 562 nm was measured by the Synergy HT Plate Reader (Biotek, Winooski, VT, USA). The samples were diluted in RIPA buffer to standardize protein concentration, and then combined with Lamelli sample buffer and boiled at 100°C for 1–3 min. In contrast to lysates of freshly isolated GCs, however, total protein of lysates of cultured GCs were quantified using the BCA assay. For electrophoresis, 10 µg of total protein was loaded into each well (25 µL total volume loaded per well), with electrophoresis, immunoblotting, and densitometric analyses of detected proteins performed in triplicate as described below.

GC proliferation assays

The GCs of small and large antral follicles were seeded at 5, 000 viable cells/well into 96 well plates (Costar, Tewksbury, MA, USA), and treated with the GFAT inhibitor, DON (50 µM), the OGT inhibitor, OSMI-1 (50 µM), or the OGA inhibitor, Thiamet-G (2.5 µM), for 24 h. Following treatment, GC proliferation was measured using the CellTiter 96® AQueous One Solution Cell Proliferation Assay (MTS) kit following manufacturer instructions (Promega, Madison, WI, USA) including the use of a Synergy HT Plate Reader (BioTek). Proliferation was measured 4 h after the addition of the MTS reagent.

GC proliferation (Ki-67 immunodetection)

The GCs from small and large antral follicles were seeded onto coverslips in 12 well plates at a density of 50, 000 viable cells/well and exposed to Thiamet-G (2.5 µM) or OSMI-1 50 (µM) for 24 h. Following treatment, the cells were washed with PBS + 0.1% BSA (Fisher Bioreagents) and then fixed with 10 mL of 100% ice-cold methanol (Fisher Scientific) and incubated at −20°C for 10 min. Fixative was removed, and the cells were washed three times with 1× PBS + 0.1% BSA. Subsequently, the coverslips with attached cells were removed from the plates and placed cell side down on blocking buffer, which consisted of 10% normal goat serum (Vector Laboratories, Burlingame, CA, USA) in 1X PBS and 0.1%BSA, and placed in an incubation chamber for 1 h. They were then incubated with rabbit anti-Ki-67 monoclonal antibody (1:200, #MA5–14520, RRID: AB_10979488 Invitrogen, Carlsbad, CA, USA) overnight at 4°C. Subsequently the coverslips were washed as described above and incubated in goat antirabbit (1:100, #sc-2004, RRID: AB_631746, Santa Cruz Biotechnology) secondary antibody for 1 h in the dark. After washing, the coverslips were incubated in ImmPACT DAB (Vector) for 10 min in the dark. The coverslips were then rinsed in cold tap water, Scott's Tap Water Solution for 1 min, and again in cold tap water. The GCs were then counterstained with hematoxylin (Vector) and washed with distilled water until clear. The coverslips were mounted onto slides using VectaMount AQ (Vector) and allowed to dry for 24 h prior to imaging. Slides were viewed and imaged using an Invitrogen EVOS M5000 microscope (Thermo Fisher, Carlsbad, CA, USA). Image analysis was conducted using the Cell Counter function on ImageJ (National Institute of Health).

Electrophoresis, immunoblotting, and densitometric analysis

Lysates of both freshly isolated and cultured GCs from small and large follicles were analyzed. Protein extracts were separated on precast, stain free 10% gels (BioRad, Hercules, CA, USA). Following electrophoretic separation, gels were activated and imaged for total protein on the BioRad ChemiDoc Imaging System. Proteins were then transferred to a PVDF membrane (BioRad) using a semi-dry transfer system at 45 mA for 1 h (Hoefer, Holliston, MA, USA). Post transfer, the gels were again imaged on the ChemiDoc Imaging System (BioRad) to verify complete transfer of the separated proteins. Following protein transfer, the PVDF membranes were blocked in Tris-buffered saline (TBS) blocking buffer containing 5% BSA and 0.2% Tween 20 (TBST; Fisher Bioreagents, Pittsburgh, PA, USA) for 3 h on a platform rocker at room temperature. Membranes were incubated overnight at 4°C with mouse anti-O-GlcNAc (1:2500, #9875, RRID: AB_10926833) or rabbit anti-OGT (1:1000, #24083, RRID: AB_2716710) primary antibodies, both from Cell Signaling

Technology (Danvers, MA, USA). Following overnight incubation, membranes were washed with TBST under agitation in the following order: 2× for 10–30 s, 1× for 15 min, and 3× for 5 min. The membranes were then incubated in secondary antibody for 1 h on a platform rocker at room temperature. Goat-antimouse (1:5000, #sc-2005, RRID: AB_631736) and goat-antirabbit (1:5000, #sc-2004, RRID: AB_631746) horseradish peroxidase conjugated secondary antibodies, respectively, were used from Santa Cruz Biotechnologies (Dallas, TX, USA). The membranes were washed as described above and were then incubated in Clarity Western ECL Blotting substrate (BioRad) for 5 min. Immunodetectable proteins were imaged on the ChemiDoc Imaging System (BioRad). After imaging, the membranes were stripped using Restore Western Blot Stripping Buffer (Thermo Scientific) per manufacturer's instructions and reprobed for OGT using the methods described above. However, the membranes were placed in blocking buffer for 3 h at room temperature prior to reprobing. O-GlcNAc and OGT protein values were normalized to total protein prior to immunoblotting as described above. Images were analyzed using Image J (National Institute of Health) for protein quantification.

Metabolite assays

Samples of follicular fluid from the small and large antral follicles used in the above experiments were assayed for concentrations of glucose and lactate. Commercially available colorimetric kits were used for measuring glucose (Sigma, St. Louis, MO, MAK263) and lactate (Sigma, MAK064) following the manufacturer's instructions, including implementation of a standard curve. For the lactate assay, dilution of the follicular fluid collected from small follicles was necessary (1:100) because lactate concentrations in undiluted samples were beyond the range of the standard curve. Absorbance at 570 nm was measured using the Synergy HT Plate Reader (Biotek) for both glucose and lactate assays.

Steroid assays

Samples of follicular fluid from the same small and large antral follicles used above were also assayed for concentrations of estradiol and progesterone. Radioimmunoassays were performed in the laboratory of Dr George Perry, South Dakota State University, using methods described previously [15]. Serial dilutions (1:10–1:100, 000) of samples were performed using 1% BSA. The intra-assay coefficients of variation were 3.84% and 4.39% for the estradiol and progesterone assays, respectively.

Statistics

A paired t-test was used to compare O-GlcNAc and OGT expression between GCs obtained from small and large follicles within the same ovary pair. Similarly, a paired t-test was used to test for differences in glycolytic components and steroids in the follicular fluid between small and large follicles of the same ovary pair. Two-tailed Pearson's correlation was used to assess the relationship between steroid and O-GlcNAcylation profiles. A repeated measures one-way ANOVA followed by Dunnett's multiple comparisons or a paired t-test were used to evaluate O-GlcNAcylation and cell proliferation relative to treatment. Ki-67 expression was analyzed with a Friedman test followed by Dunn's multiple comparisons. Significant differences were declared at $P < 0.05$. Tests were performed using GraphPad Prism 8 statistical software.

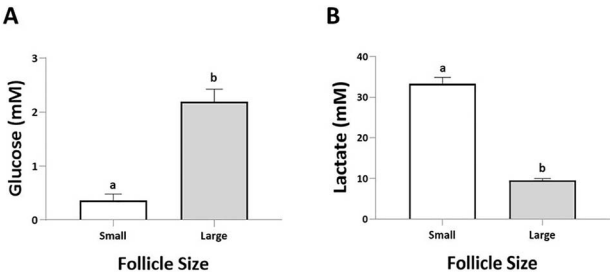

Figure 2. Relative concentrations of glucose and lactate in follicular fluid of bovine antral follicles according to follicle size. (**A**) Glucose concentrations and (**B**) lactate concentrations are depicted for small (SF; 3–5 mm) and large (LF; >10 mm) bovine follicles. Results represent $n = 7$ ovary pairs, run in duplicate, with the mean ± SEM concentration (mM) of a given metabolite shown. Different letters denote differences between SF and LF at $P < 0.05$.

Results

Glucose and lactate concentrations in follicular fluid differ by follicle size

The metabolic status of the follicles was assessed by determining the relative glucose and lactate concentrations of the follicular fluid via colorimetric assay. Analysis of the follicular fluid of small and large follicles within the same ovary pair indicated differences in glucose and lactate concentrations. As shown in Figure 2, large follicles had higher glucose concentrations (Figure 2A; $P < 0.05$), but lower lactate concentrations (Figure 2B; $P < 0.05$) than small follicles. Notably, even though lactate concentrations were lower in large follicles compared to small follicles, the amount of lactate in the follicular fluid of both sizes of follicles was at least 10 times greater than glucose concentrations (Compare Y-axis of Figure 2A versus Figure 2B).

Both small and large follicles have high P4:E2 ratios

Relative health of the follicles from the slaughterhouse ovaries was assessed by analyzing the estradiol and progesterone concentrations in the follicular fluid by radioimmunoassay. In all 7 pools of small follicles analyzed, the ratio of progesterone (P4) to estradiol (E2) concentration in the follicular fluid exceeded a factor of 10 (>10). Similarly, five of the seven large follicles had a P4/E2 ratio > 10, whereas the remaining two had an intermediate ratio of greater than 1 (>1), but less than 10 (<10). The average E2 concentration in the follicular fluid of small follicles was 1.60 ng/mL (Range: 0.10–6.34 ng/mL); whereas for large follicles it was 13.4 ng/mL (Range: 0.199–55.9 ng/mL). Conversely, the average P4 concentration in the follicular fluid of small follicles was 130.5 ng/mL, (range: 38.5–470.9 ng/mL); whereas for large follicles it was 157 ng/mL, (range: 19.8–377 ng/mL). Regardless, the GCs obtained from all of these follicles were viable and used in all subsequent experiments. There was no correlative pattern observed between the relative P4:E2 ratio for a given follicle size classification and the amount of immunodetectable O-GlcNAcylation measured from the GCs therein ($P > 0.05$, $r = 0.2$ and $r = 0.1$ for small and large follicles, respectively).

Global O-GlcNAcylation and OGT expression in bovine GCs differs by follicle size

Evidence of O-GlcNAcylation in freshly isolated bovine GCs was determined by immunodetection (Figure 3A). The expression of global O-GlcNAcylation and OGT in GCs of small versus large antral follicles differed within the same ovary pair (Figure 3A).

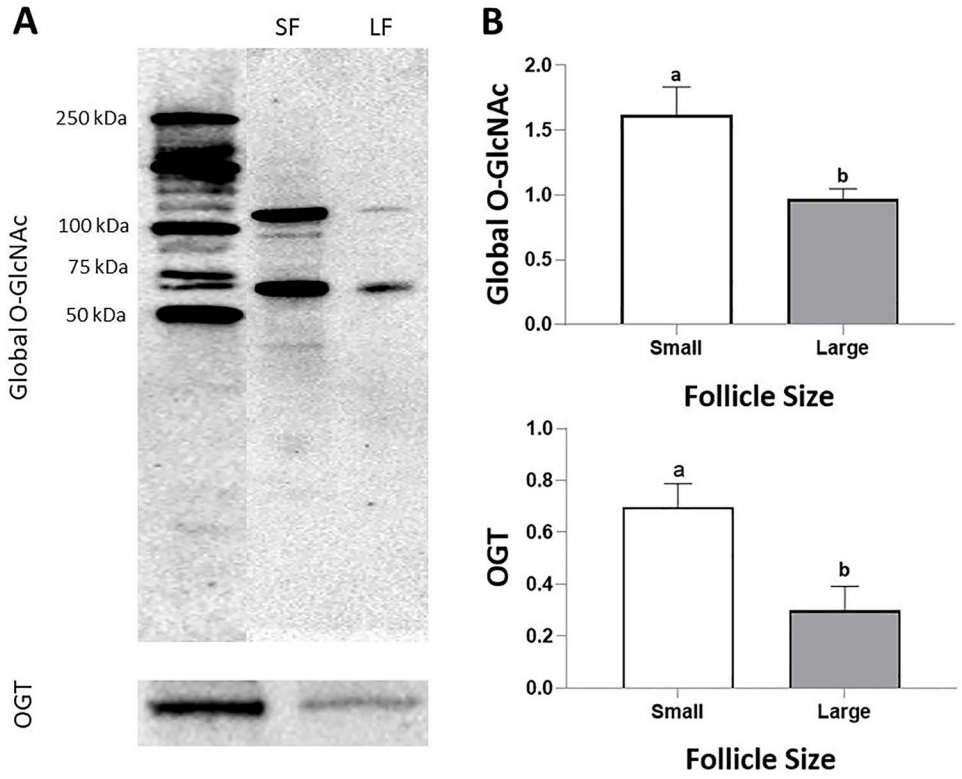

Figure 3. Immunoblots and measurement of global O-GlcNAcylation and OGT expression in freshly isolated bovine granulosa cells of small and large antral follicles. (**A**) Immunoblot of global O-GlcNAcylation and OGT expression (MW:110 kDa) in freshly isolated bovine granulosa cells of small (SF; 3–5 mm) and large (LF; >10 mm) follicles. (**B**) Bar graphs of the densitometric analysis of O-GlcNAcylated proteins and OGT expression relative to total protein expression. Results represent $n = 7$ ovary pairs run in triplicate, with the mean ± SEM signal intensity shown. Different letters denote differences between SF and LF at $P < 0.05$.

Overall, GCs obtained from small follicles had greater expression of global O-GlcNAcylation (Figure 3B; $P < 0.05$) and OGT (Figure 3B; $P < 0.05$) than GCs of large follicles.

Disruption of O-GlcNAcylation impairs GC proliferation

The role of O-GlcNAcylation was further assessed by determining its effects on bovine GC proliferation, as measured by MTS assay and immunodetection of Ki-67. As shown in Figure 4, the GFAT inhibitor, DON, prevented O-GlcNAcylation in GCs from small follicles (Figure 4A and B; $P < 0.05$) and large follicles (Figure 4D and E; $P < 0.05$). The inhibition of O-GlcNAcylation impaired GC proliferation, regardless of follicle size (Figure 4C and F for small and large follicles, respectively; $P < 0.05$). As shown in Figure 5, a time-course experiment revealed that the small molecule inhibitor of OGT, OSMI-1, similarly impaired O-GlcNAcylation in GCs of small follicles at 4 and 8 h (Figure 5A and B; $P < 0.05$), but failed to sustain this effect at 12 and 24 h (Figure 5A and B; $P > 0.05$). Nevertheless, inhibition of O-GlcNAcylation via OSMI-1 impaired proliferation of GCs from small follicles (Figure 5 C; $P < 0.05$). Conversely, OSMI-1 had no effect on O-GlcNAcylation in GCs of large follicles, regardless of time of treatment (Figure 5D and E; $P > 0.05$), and had no effect on GC proliferation (Figure 5F; $P > 0.05$). As shown in Figure 6, augmentation of O-GlcNAcylation via the small molecule inhibitor of OGA, Thiamet-G, enhanced O-GlcNAcylation in the GCs of both follicle sizes (Figure 6A and B, and Figure 6D and E, for small and large follicles, respectively; $P < 0.05$), but had no effect on GC proliferation in either size of follicle (Figure 6C and F, for small and large follicles, respectively; $P > 0.05$).

Additional effects of these small molecule inhibitors on GC proliferation were assessed by immunocytochemistry. As shown in Figure 7, OSMI-1 reduced the number of Ki-67 positive cells compared to control and Thiamet-G-treated GCs of small follicles (Figure 7A and C; $P < 0.05$), but there was no effect of OSMI-1 or Thiamet-G on numbers of Ki-67 positive GCs of large follicles (Figure 7B and C; $P > 0.05$).

Discussion

Glucose utilization in the context of O-GlcNAcylation and bovine GC metabolism was evaluated in the current study. We present clear evidence that O-GlcNAcylation occurs in bovine GCs, and that this process is regulated by the HBP through the enzymatic actions of GFAT, OGT, and OGA (Figure 1). Global O-GlcNAcylation was evident in GCs of both small and large antral follicles, but with a greater degree of O-GlcNAcylation detectable in GCs from small follicles. Interestingly, the follicular fluid of small follicles also contained less glucose (Figure 2), suggesting that a greater proportion of available glucose is metabolized in these follicles, shunted toward the HBP and utilized for O-GlcNAcylation. Rapid glucose metabolism is often indicative of glycolytic processes, rather than oxidative phosphorylation [16], and this concept is supported in the current study by the observation that small antral follicles also contained a greater proportion of lactate (Figure 2), a product of glycolytic metabolism.

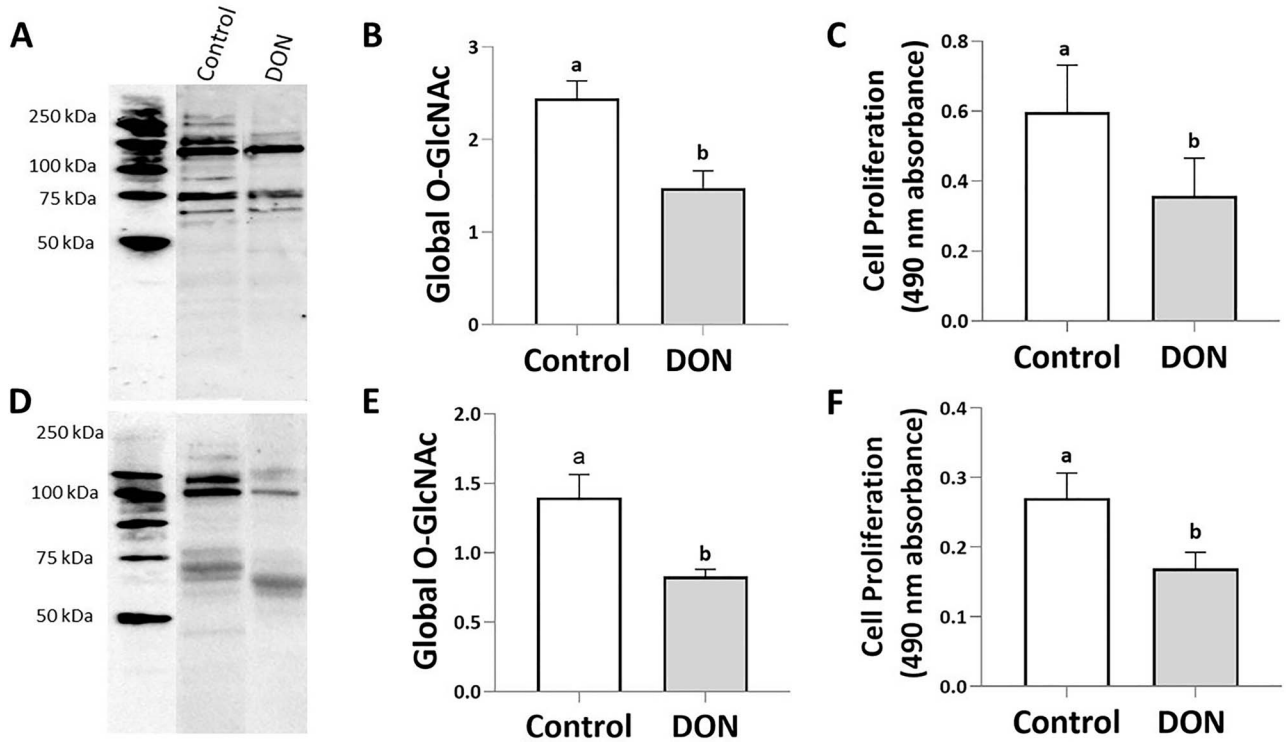

Figure 4. Immunoblots, measurement of global O-GlcNAcylation, and quantification of cell proliferation following treatment of cultured bovine granulosa cells from small and large antral follicles with the glutamine fructose-6-phosphate aminotransferase (GFAT) inhibitor, DON. (**A–C**) Effects of 24-hour exposure to DON (50 μM) on global O-GlcNAcylation (**A, B**) and granulosa cell proliferation (**C**) in cells from small antral follicles (3–5 mm). (**D–F**) Effects of 24-hour exposure to DON (50 μM) on global O-GlcNAcylation (**D, E**) and granulosa cell proliferation (**F**) in cells from large antral follicles (>10 mm). Representative immunoblots and corresponding bar graphs of the densitometric analyses of global O-GlcNAcylation relative to total protein for the two follicle sizes (**A** and **B**, **D** and **E**) are shown. Bar graphs depicting granulosa cell proliferation as measured by MTS assay for the two follicle sizes (**C** and **F**) are also shown. Results representative of $n = 4$–5 independent experiments run in triplicate, with the mean ± SEM signal intensity or absorbance at 490 nm indicated. Different letters denote differences from control at $P < 0.05$.

Similar findings of glycolytic metabolism in GCs of other species are evident. For instance, in sheep, glucose is metabolized to lactate and is the preferred pathway for gonadotropin-induced differentiation of GCs [17]. Similarly, in pigs, GCs of small antral follicles undergo rapid cell proliferation, and this is accompanied by a metabolic shift toward aerobic glycolysis, a phenomenon known as the Warburg Effect [18]. The Warburg Effect is characteristic of rapidly proliferating cells, particularly cancer cells, wherein accelerated conversion of glucose to lactate results [19]. The Warburg Effect is also mechanistically linked to O-GlcNAcylation because several glycolytic enzymes involved (e.g., phosphofructokinase 1 and enolase) are also targets of O-GlcNAcylation [20, 21]. O-GlcNAcylation of these enzymes can impair their activity, potentially influencing metabolic shifts within the cell [21]. Thus, the observation of O-GlcNAcylation within bovine GCs, coupled with the evidence of glycolytic metabolism, is significant and could have an important role in influencing GC function.

In the current study, as antral follicle size increased, glucose concentrations accumulating within the follicular fluid also increased (Figure 2). Conversely, lactate concentrations decreased (Figure 2). The concentrations of carbohydrates reported here are similar to what others have observed previously [16, 22]. These observations are also consistent with current thinking about the prevailing form of metabolism taking place as bovine antral follicles grow during folliculogenesis [22–24]. Specifically, relative concentrations of glucose and lactate in the follicular fluid are attributed to enhanced glucose uptake and glycolytic metabolism within small follicles, that later diminishes as the follicles increase in size and maturity [22, 23]. Alternatively, as follicles grow, the permeability of the blood-follicle barrier also increases, which alters metabolite concentrations to the point of being similar to that of blood serum in systemic circulation [25, 26]. Our results are consistent with the concept that GCs of small follicles exhibit glycolytic metabolism (i.e., the Warburg Effect), conducive to rapid cell proliferation. Enhanced glucose uptake and glycolytic metabolism are compatible with the greater extent of O-GlcNAcylation observed in the GCs of small follicles, presumably as they shunt excess glucose toward the HBP. Conversely, increased glucose accumulation in the follicular fluid of large follicles, accompanied by less lactate (Figure 2), suggests GCs of these follicles metabolically transition to oxidative phosphorylation, wherein glucose becomes completely oxidized. Indeed, the observation of diminished O-GlcNAcylation in the GCs of large follicles (Figure 3) hints there is less available glucose to shunt to the HBP. Collectively, the above observations offer a scenario in which O-GlcNAcylation and glycolytic metabolism could favor GC proliferation (small antral follicles); whereas oxidative phosphorylation and diminished O-GlcNAcylation support GC function and differentiation (large antral follicles). Initial evidence in support of this scenario is presented here, wherein inhibition of O-GlcNAcylation (via DON or OSMI-1) prevented proliferation of GCs from small antral follicles (Figures 4–6).

The concept that O-GlcNAcylation and glucose metabolism influence GC function is borne out by experiments in the current

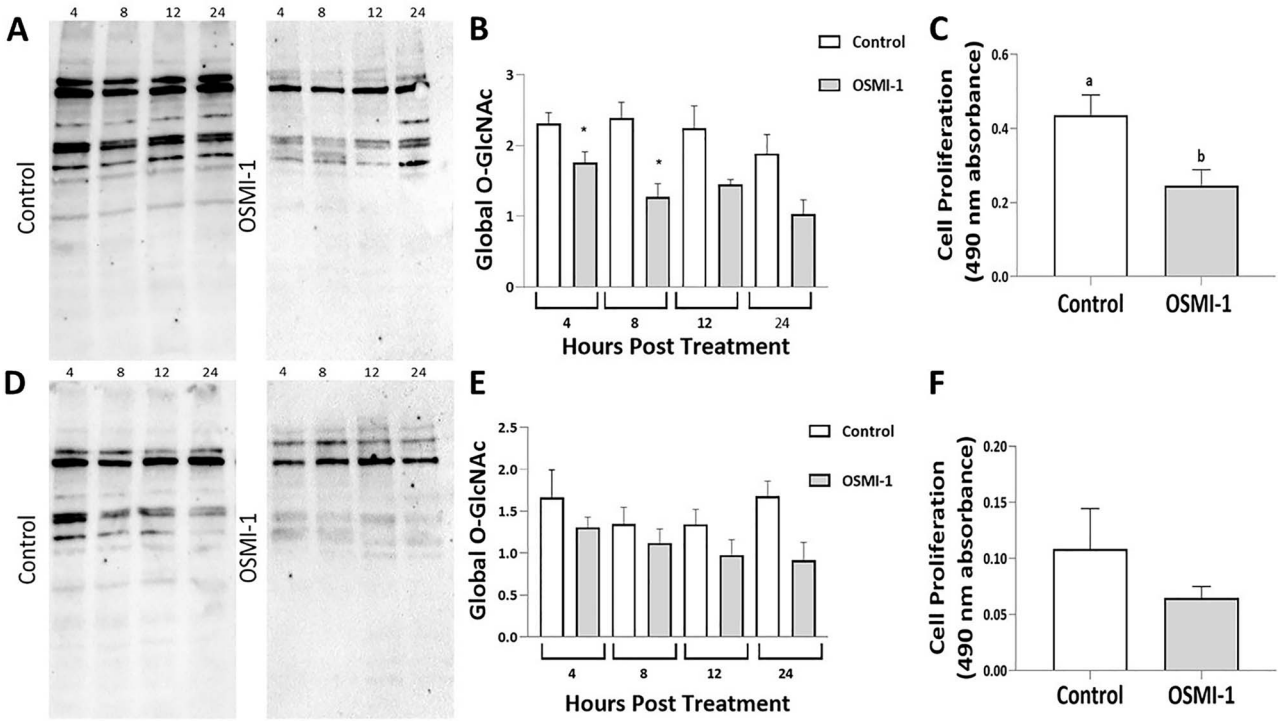

Figure 5. Immunoblots, measurement of global O-GlcNAcylation, and quantification of cell proliferation following time-course treatment of cultured bovine granulosa cells from small and large antral follicles with the O-GlcNAc transferase (OGT) inhibitor, OSMI-1. (**A–C**) Effects of OSMI-1(50 μM) on global O-GlcNAcylation after 4, 8, 12, and 24 h of exposure to the inhibitor (**A, B**); and on granulosa cell proliferation after 24 h of exposure to the inhibitor (**C**) in cells from small antral follicles (3–5 mm). (**D–F**) Effects of OSMI-1 (50 μM) on global O-GlcNAcylation after 4, 8, 12, and 24 h of exposure to the inhibitor (**D, E**); and on granulosa cell proliferation after 24 h of exposure to the inhibitor (**F**) in cells from large antral follicles (>10 mm). Representative immunoblots and corresponding bar graphs of the densitometric analyses of global O-GlcNAcylation relative to total protein for the two follicle sizes (**A** and **B**, **D** and **E**) are shown. Bar graphs depicting granulosa cell proliferation as measured by MTS assay for the two follicle sizes (**C** and **F**) are also shown. Results represent $n = 3–6$ independent experiments run in triplicate, with the mean ± SEM signal intensity or absorbance at 490 nm indicated. Different letters or asterisks denote differences from control at $P < 0.05$.

investigation in which disrupting the HBP directly, or selectively influencing endogenous O-GlcNAc cycling, altered GC proliferation. Specifically, the rate limiting step of glucose processing through the HBP, the GFAT enzyme, influences the synthesis of all downstream intermediates, including the formation of UDP-GlcNAc for O-GlcNAcylation (Figure 1). In the present study, direct inhibition of GFAT prevented O-GlcNAcylation and inhibited proliferation of GCs from both small and large antral follicles (Figure 4). These results were expected, in part because a loss of O-GlcNAcylation at this level impairs proliferation of even the most rapidly dividing cells, including cancer cells and other immortal cell lines [27, 28]. However, when inhibition of O-GlcNAcylation occurred more directly, via the OGT inhibitor, OSMI-1, only proliferation of GCs from small follicles was measurably compromised (Figure 5). We interpret this outcome as being a consequence of the GCs of small follicles having greater capacity to divide than GCs of large follicles. This thinking is also consistent with the GCs having a prominent role in the ability of the follicle to grow during folliculogenesis. Conversely, GCs of large follicles are presumably nearing the stages of terminal differentiation or luteinization, wherein cell division is less frequent [29, 30], acquisition of LH receptors occurs [31–33], and resistance to apoptosis becomes attainable [34]. Indeed, under culture conditions, we and others have found that GCs typically obtained from small antral follicles exhibit greater rates of proliferation, with a shorter generation interval, and are less prone to spontaneous luteinization than GCs obtained from larger follicles [20, 35, 36, unpublished observations and supplementary information]. In the current study, GC proliferation was measured by both mitochondrial activity (MTS assay) and the cell proliferation marker, Ki-67 (immunodetection), which is only expressed by dividing cells. The lack of O-GlcNAcylation (via DON and OSMI-1 treatment) prevented cell proliferation by impeding aspects of both mitochondrial activity and cell cycle regulation (Figures 4–6).

Enhancement of O-GlcNAcylation, or hyper-O-GlcNAcylation, is associated with increased cell proliferation and amplified tumorigenic potential [36, 37]. Specifically, hyper-O-GlcNAcylation enhances cancer cell aggressiveness through increased expression of epithelial-mesenchymal transition genes, stimulating cell proliferation, and enhancing cell migration and/or invasiveness [36]. In contrast, a diminishment of O-GlcNAcylation, or hypo-O-GlcNAcylation, impairs these measures [36]. Additional evidence supporting the concept that some degree of O-GlcNAcylation is necessary for cell homeostasis comes from genetic knockout experiments, in which knockout of the OGT enzyme results in an embryonic lethal phenotype [38]. Conversely, OGA knockouts are less phenotypically severe: there is lethality in the neonatal mouse, but the detrimental effects include growth defects, mitotic defects, binucleation, and chromosome lagging [39]. In the current study, hyper-O-GlcNAcylation (via Thiamet-G) had no effect on GC proliferation from either small or large antral follicles (Figure 6). It is conceivable that GCs from small follicles already metabolize glucose and proliferate at such rapid rates that further stimulation of

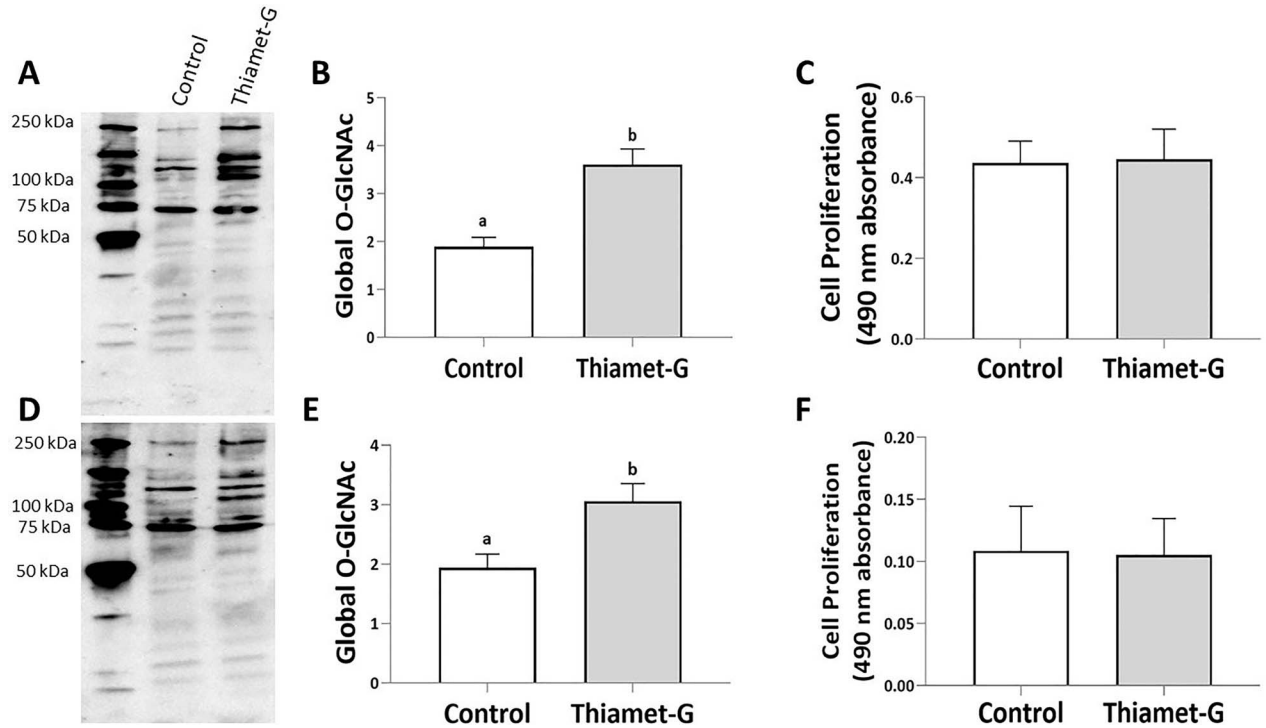

Figure 6. Immunoblots, measurement of global O-GlcNAcylation, and quantification of cell proliferation following treatment of cultured bovine granulosa cells from small and large antral follicles with the O-GlcNAcase (OGA) inhibitor, Thiamet-G. (**A–C**) Effects of 24 h exposure to Thiamet-G (2.5 μM) on global O-GlcNAcylation (**A, B**) and granulosa cell proliferation (**C**) in cells from small antral follicles (3–5 mm). (**D, E, F**) Effects of 24 h exposure to Thiamet-G (2.5 μM) on global O-GlcNAcylation (**D, E**) and granulosa cell proliferation (**F**) in cells from large antral follicles (>10 mm). Representative immunoblots and corresponding bar graphs of the densitometric analyses of global O-GlcNAcylation relative to total protein for the two follicle sizes (**A** and **B**, **D** and **E**) are shown. Bar graphs depicting granulosa cell proliferation as measured by MTS assay for the two follicle sizes (**C** and **F**) are also shown. Results represent $n = 3–6$ independent experiments run in triplicate, with the mean ± SEM signal intensity or absorbance at 490 nm shown indicated. Different letters denote differences from control at $P < 0.05$.

these activities via O-GlcNAcylation is unattainable experimentally. On the other hand, GCs of large follicles perhaps have become committed to their terminal fate (i.e., apoptosis, luteinization), and thus are resistant to further alterations of glucose metabolism involving the HBP. These issues merit further investigation.

The current study is the first to detect and characterize O-GlcNAcylation in GCs of bovine antral follicles, but others have reported the existence of OGT and OGA enzymes, and expression of O-GlcNAcylated proteins, in cumulus oocyte complexes (COCs) [40]. Hyper-O-GlcNAcylation (via Thiamet-G), has no detrimental effects on the cumulus cells or the oocyte, but zygote formation following in vitro fertilization is compromised [40]. Other investigations report, however, that increased glucose shunting through the HBP (thus potentiating O-GlcNAcylation) has deleterious effects on oocyte health and developmental competence. For instance, glucosamine is a direct substrate for the HBP and perturbs post-compaction development of bovine and murine embryos [41, 42]. Inhibiting O-GlcNAcylation reverses these detrimental effects [42]. Supplementation of glucosamine to mouse COCs increases HSP90 expression, an effect reversed by using BADGP (an OGA inhibitor), and is associated with decreased oocyte competence. [43]. Complete inhibition of the HBP and O-GlcNAcylation via DON, however, prevents cumulus expansion [43, 44]. Collectively, these observations suggest O-GlcNAcylation is essential to some of the major constituents of the growing follicle (i.e., GCs, cumulus cells, and oocyte), and helps support their growth, health, and developmental competence in a homeostatic manner.

There is growing, albeit limited, evidence that O-GlcNAcylation may exert direct effects within reproductive tissues through classical steroid signaling pathways. For instance, estrogen receptors (ER) α and β are both heavily O-GlcNAcylated [45, 46]. Cancer therapies that induce O-GlcNAcylation also inhibit ER α expression [47]. In contrast, O-GlcNAcylation of the ER β maintains its stability and its transcriptional actions [46, 48]. Although these studies are somewhat limited in scope, they nevertheless provide credibility to the concept that O-GlcNAcylation modulates the actions of steroids, and thus may influence steroid receptor-mediated aspects of ovarian function, including folliculogenesis and oocyte maturation.

Conclusion

In conclusion, the mechanism(s) by which O-GlcNAcylation influences GC function in bovine antral follicles is not understood at the current time, but offers fertile ground for further investigation. Our study demonstrated that differences in glucose and lactate accumulation within the follicular fluid as follicles grow mirror the relative state of O-GlcNAcylation within the GCs, and likely the relative magnitude of glucose metabolism taking place. GCs of small follicles exhibit greater expression of O-GlcNAcylation than those of large follicles, ostensibly because glucose is more readily utilized and metabolized glycolytically to support cell proliferation (i.e., the Warburg Effect). The results supported the hypothesis that O-GlcNAcylation differs in GCs according to antral follicle size and

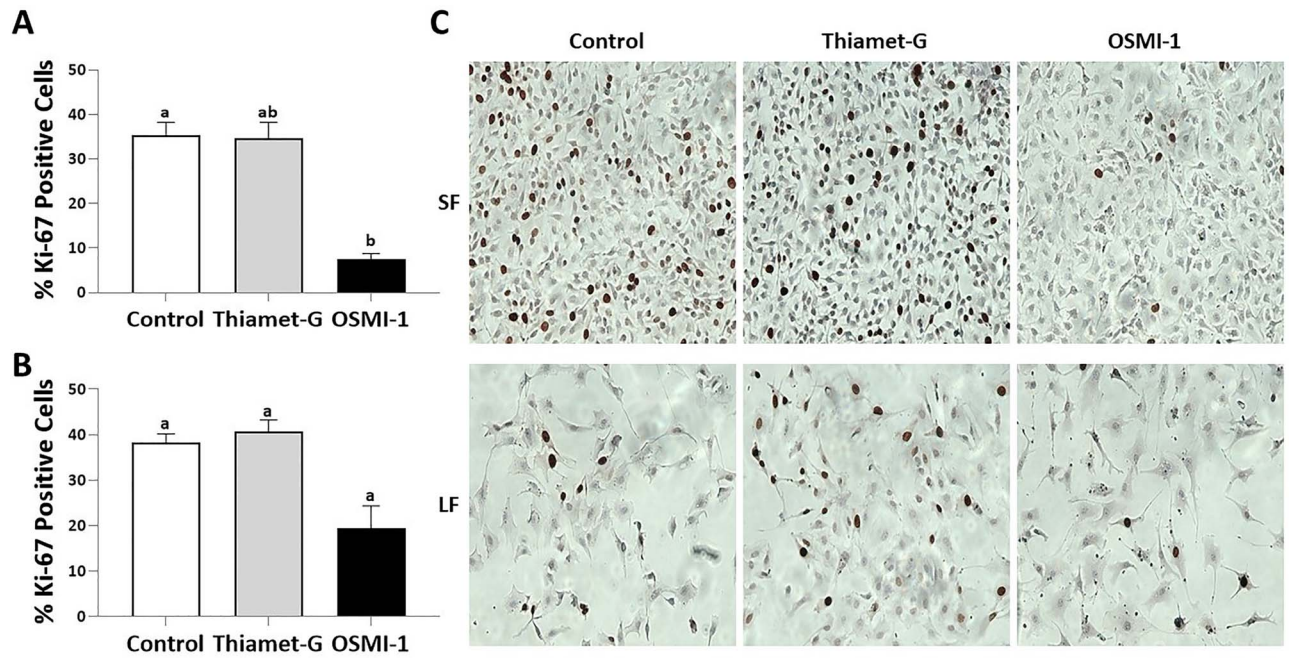

Figure 7. Immunodetection of granulosa cell proliferation (via Ki-67 staining) following augmentation and inhibition of O-GlcNAcylation with Thiamet-G (2.5 μM) and OSMI-1 (50 μM), respectively. Bar graphs depicting the percentage of Ki-67 positive cells from small antral follicles (SF, 3–5 mm; **A**) and large antral follicles (LF, >10 mm; **B**) are shown. (**C**) Representative photomicrographs (Bar = 150 μm) depicting Ki-67 staining (darkened cells) in cultured bovine granulosa cells of small and large antral follicles (SF and LF, respectively) following 24-hour treatment with DMSO (control), Thiamet-G, and OSMI-1. Results represent $n = 5$ independent experiments, run in duplicate, with the mean ± SEM of Ki-67 expression shown. Different letters denote differences among treatments at $P < 0.05$.

ultimately influences GC proliferation. Observing that downregulation of O-GlcNAcylation impairs GC proliferation, this may become important as follicles reach maturity and GCs begin to undergo differentiation (e.g., luteinization). Future studies should determine the identity of key O-GlcNAcylated proteins in the follicle, the effects of O-GlcNAcylation on steroidogenesis and steroid action in the follicle, and the role of O-GlcNAcylation as a potential nutrient sensor in folliculogenesis.

Conflict of interest

The authors have declared that no conflict of interest exists.

Authors' contributions

AMM and DHT conceived the study, experimental design, and wrote the manuscript. AMM performed the experiments and conducted the statistical analyses.

Acknowledgments

Portions of this work were presented previously at the Réseau Québécois en reproduction Symposium 2019 in Quebec City, Canada, and the 53rd Annual Meeting of the Society for the Study of Reproduction (virtual meeting, July, 2020). We are grateful to Dr. George Perry and his laboratory at South Dakota State University for the steroid analyses conducted in this study.

References

1. Bond MR, Hanover JA. A little sugar goes a long way: the cell biology of O-GlcNAc. *J Cell Biol* 2015; **208**:869–880.
2. Comer FI, Hart GW. O-glycosylation of nuclear and cytosolic proteins. Dynamic interplay between O-GlcNAc and O-phosphate. *J Biol Chem* 2000; **275**:29179–29182.
3. Hardivillé S, Hart GW. Nutrient regulation of signaling, transcription, and cell physiology by O- GlcNAcylation. *Cell Metab* 2014; **20**:208–213.
4. Hardie DG, Ross FA, Hawley SA. AMPK: A nutrient and energy sensor that maintains energy homeostasis. *Nat Rev Mol Cell Biol* 2012; **13**:251–262.
5. Efeyan A, Comb WC, Sabatini DM. Nutrient-sensing mechanisms and pathways. *Nature* 2015; **517**:302–310.
6. Hart GW, Slawson C, Ramirez-Correa G, Lagerlof O. Cross talk between O-GlcNAcylation and phosphorylation: roles in signaling, transcription, and chronic disease. *Annu Rev Biochem* 2011; **80**:825–858.
7. Chatham J, Marchase R. Protein O-GlcNAcylation: a critical regulator of the cellular response to stress. *Curr Signal Transduct Ther* 2010; **5**:49–59.
8. Dias WB, Cheung WD, Hart GW. O-GlcNAcylation of kinases. *Biochem Biophys Res Commun* 2012; **422**:224–228.
9. Tosca L, Froment P, Solnais P, Ferré P, Foufelle F, Dupont J. Adenosine 5′-monophosphate-activated protein kinase regulates progesterone secretion in rat granulosa cells. *Endocrinology* 2005; **146**:4500–4513.
10. Tosca L, Ramé C, Chabrolle C, Tesseraud S, Dupont J. Metformin decreases IGF1-induced cell proliferation and protein synthesis through AMP-activated protein kinase in cultured bovine granulosa cells. *Reproduction* 2010; **139**:409–418.
11. Tosca L, Solnais P, Ferré P. FF-B of, 2006 U. Metformin-induced stimulation of adenosine 5′ monophosphate-activated protein kinase (PRKA) impairs progesterone secretion in rat granulosa cells. *Biol Reprod* 2006; **75**:342–351.
12. Kayampilly PP, Menon KMJ. Follicle-stimulating hormone inhibits adenosine 5′-monophosphate-activated protein kinase activation and promotes cell proliferation of primary Granulosa cells in culture through an Akt-dependent pathway. *Endocrinology* 2009; **150**:929–935.
13. Campbell BK, Scaramuzzi RJ, Webb R. Control of antral follicle development and selection in sheep and cattle. *J Reprod Fertil Suppl* 1995; **49**:335–350.

14. Yaba A, Bianchi V, Borini A, Johnson J. A putative mitotic checkpoint dependent on mTOR function controls cell proliferation and survival in ovarian granulosa cells. *Reprod Sci* 2008; **15**:128–138.
15. Perry GA, Perry BL. Effect of preovulatory concentrations of estradiol and initiation of standing estrus on uterine pH in beef cows. *Domest Anim Endocrinol* 2008; **34**:333–338.
16. Nandi S, Girish Kumar V, Manjunatha BM, Ramesh HS, Gupta PSP. Follicular fluid concentrations of glucose, lactate and pyruvate in buffalo and sheep, and their effects on cultured oocytes, granulosa and cumulus cells. *Theriogenology* 2008; **69**:186–196.
17. Campbell BK, Onions V, Kendall NR, Guo L, Scaramuzzi RJ. The effect of monosaccharide sugars and pyruvate on the differentiation and metabolism of sheep granulosa cells in vitro in: Reproduction Volume 140 Issue 4 (2010). *Reproduction* 2010; **140**:541–550.
18. Costermans NGJ, Keijer J, van Schothorst EM, Kemp B, Keshtkar S, Bunschoten A, Soede NM, Teerds KJ. In ovaries with high or low variation in follicle size, granulosa cells of antral follicles exhibit distinct size-related processes. *Mol Hum Reprod* 2019; **25**:614–624.
19. Warburg O. The metabolism of carcinoma cells 1. *J Cancer Res* 1925; **9**:148–163.
20. Yi W, Clark PM, Mason DE, Keenan MC, Hill C, Goddard WA, Peters EC, Driggers EM, Hsieh-Wilson LC. Phosphofructokinase 1 glycosylation regulates cell growth and metabolism. *Science (80-)* 2012; **337**:975–980.
21. Champattanachai V, Netsirisawan P, Chaiyawat P, Phueaouan T, Charoenwattanasatien R, Chokchaichamnankit D, Punyarit P, Srisomsap C, Svasti J. Proteomic analysis and abrogated expression of *O* -GlcNAcylated proteins associated with primary breast cancer. *Proteomics* 2013; **13**:2088–2099.
22. Leroy JLMR, Vanholder T, Delanghe JR, Opsomer G, Van Soom A, Bols PEJ, De Kruif A. Metabolite and ionic composition of follicular fluid from different-sized follicles and their relationship to serum concentrations in dairy cows. *Anim Reprod Sci* 2004; **80**:201–211.
23. Orsi NM, Gopichandran N, Leese HJ, Picton HM, Harris SE. Fluctuations in bovine ovarian follicular fluid composition throughout the oestrous cycle. *Reproduction* 2005; **129**:219–228.
24. Nandi S, Kumar VG, Manjunatha BM, Gupta PSP. Biochemical composition of ovine follicular fluid in relation to follicle size. *Dev Growth Differ* 2007; **49**:61–66.
25. Edwards RG. Follicular Fluid. *J Reprod Fertil* 1972; **37**:182–219.
26. Bagavandoss P, Midgley AR, Wicha M. Developmental changes in the ovarian follicualr basal lamina detected by immunofluorescence and electron microscopy. *J Histochem Cytochem* 1983; **31**: 633–640.
27. Steenackers A, Olivier-Van Stichelen S, Baldini SF, Dehennaut V, Toillon R-A, Le Bourhis X, El Yazidi-Belkoura I, Lefebvre T. Silencing the nucleocytoplasmic O-GlcNAc transferase reduces proliferation, adhesion, and migration of cancer and fetal human colon cell lines. *Front Endocrinol (Lausanne)* 2016; **7**:46.
28. Jaskiewicz, Nicole M, Hermawan C, Parisi S, Townson DH. O-GlcNAcylation enhances the tumorigenic properties of cervical cancer cells in vitro. *Clin Obstet Gynecol Reprod Med* 2017; **3**:1–6.
29. Ali A, Lange A, Gilles M, Glatzel PS. Morphological and functional characteristics of the dominant follicle and corpus luteum in cattle and their influence on ovarian function. *Theriogenology* 2001; **56**: 569–576.
30. Girard A, Dufort I, Douville G, Sirard MA. Global gene expression in granulosa cells of growing, plateau and atretic dominant follicles in cattle. *Reprod Biol Endocrinol* 2015; **13**:17.
31. Ireland JJ, Roche JF. Development of nonovulatory antral follicles in heifers: changes in steroids in follicular fluid and receptors for gonadotropins. *Endocrinology* 1983; **112**:150–156.
32. Ginther OJ, Bergfelt DR, Kulick LJ, Kot K. Selection of the dominant follicle in cattle: Establishment of follicle deviation in less than 8 hours through depression of FSH concentrations. *Theriogenology* 1999; **52**:1079–1093.
33. Bodensteiner KJ, Wiltbank MC, Bergfelt DR, Ginther OJ. Alterations in follicular estradiol and gonadotropin receptors during development of bovine antral follicles. *Theriogenology* 1996; **45**:499–512.
34. Jolly PD, Tisdall DJ, Heath DA, Lun S, Mcnatty KP. Apoptosis in bovine granulosa cells in relation to steroid synthesis, cyclic adenosine 3′,5′-monophosphate response to follicle-stimulating hormone and luteinizing hormone, and follicular atresia. *Biol Reprod* 1994; **51**:934–944.
35. Ledwitz-Rigby F, Rigby BW, Gay VL, Stetson M, Young J, Channing CP. Inhibitory action of porcine follicular fluid upon granulosa cell luteinization in vitro: assay and influence of follicular maturation. *J Endocrinol* 1977; **74**:175–184.
36. Jaskiewicz NM, Townson DH. Hyper-O-GlcNAcylation promotes epithelial-mesenchymal transition in endometrial cancer cells. *Oncotarget* 2019; **10**:2899–2910.
37. Liu Q, Tao T, Liu F, Ni R, Lu C, Shen A. Hyper-O-GlcNAcylation of YB-1 affects Ser102 phosphorylation and promotes cell proliferation in hepatocellular carcinoma. *Exp Cell Res* 2016; **349**:230–238.
38. Shafi R, Prasad S, Iyer N, Ellies LG, O'donnell N, Marek KW, Chui D, Hart GW, Marth JD, Palade GE. The O-GlcNAc transferase gene resides on the X chromosome and is essential for embryonic stem cell viability and mouse ontogeny. *Proc Natl Acad Sci* 2000; **97**:5735–5739.
39. Yang YR, Song M, Lee H, Jeon Y, Choi E-J, Jang H-J, Moon HY, Byun H-Y, Kim E-K, Kim DH, Lee MN, Koh A et al. O-GlcNAcase is essential for embryonic development and maintenance of genomic stability. *Aging Cell* 2012; **11**:439–448.
40. Zhou LT, Romar R, Pavone ME, Soriano-Úbeda C, Zhang J, Slawson C, Duncan FE. Disruption of O-GlcNAc homeostasis during mammalian oocyte meiotic maturation impacts fertilization. *Mol Reprod Dev* 2019; **86**:543–557.
41. Schelbach CJ, Kind KL, Lane M, Thompson JG. Mechanisms contributing to the reduced developmental competence of glucosamine-exposed mouse oocytes. *Reprod Fertil Dev* 2010; **22**:771.
42. Sutton-Mcdowall ML, Mitchell M, Cetica P, Dalvit G, Pantaleon M, Lane M, Gilchrist RB, Thompson JG. Glucosamine supplementation during in vitro maturation inhibits subsequent embryo development: possible role of the hexosamine pathway as a regulator of developmental competence 1. *Biol Reprod* 2006; **74**:881–888.
43. Frank LA, Sutton-McDowall ML, Brown HM, Russell DL, Gilchrist RB, Thompson JG. Hyperglycaemic conditions perturb mouse oocyte in vitro developmental competence via beta-O-linked glycosylation of heat shock protein 90. *Hum Reprod* 2014; **29**:1292–1303.
44. Gutnisky C, Dalvit GC, Pintos LN, Thompson JG, Beconi MT, Cetica PD. Influence of hyaluronic acid synthesis and cumulus mucification on bovine oocyte in vitro maturation. *fertilisation and embryo development. Reprod Fertil Dev* 2007; **19**:488–497.
45. Cheng X, Hart GW. Glycosylation of the murine estrogen receptor-α. *J Steroid Biochem Mol Biol* 2000; **75**:147–158.
46. Cheng X, Hart GW. Alternative O-glycosylation/O-phosphorylation of Serine-16 in murine estrogen receptor β: Post-translational regulation of turnover and transactivation activity. *J Biol Chem* 2001; **276**: 10570–10575.
47. Kanwal S, Fardini Y, Pagesy P, N'Tumba-Byn T, Pierre-Eugène C, Masson E, Hampe C, Issad T. O-GlcNAcylation-inducing treatments inhibit estrogen receptor α expression and confer resistance to 4-OH-tamoxifen in human breast cancer-derived MCF-7 cells. *PLoS One* 2013; **8**:e69150.
48. Hart GW, Sakabe K. Fine-tuning ER-β structure with PTMs. *Chem Biol* 2006; **13**:923–924.